

# Study of thermal behavior of CrO<sub>3</sub> using TG and DSC

S. A. A. Sajadi · M. Khaleghian

Received: 4 May 2013 / Accepted: 15 December 2013 / Published online: 9 January 2014  
© Akadémiai Kiadó, Budapest, Hungary 2014

**Abstract** Using two techniques of thermogravimetry and differential scanning calorimetry under O<sub>2</sub> and N<sub>2</sub> gas atmosphere from 25 to 600 °C, the thermal behavior of chromium(VI) oxide CrO<sub>3</sub> was investigated. The identity of products at different decomposition steps was confirmed by XRD technique. Both techniques produced similar results supporting the same steps for the compound. The received products were investigated by SEM electron microscope. The form and the size of crystals were investigated. Three distinct energy changes were observed, namely, two endothermic and one exothermic in DSC. The amount of  $\Delta H$  for each peak is also reported.

**Keywords** Chromium(VI) oxide · TG · DSC · XRD

## Introduction

Due to their chemical and physical characteristics, chromium compounds are used in a wide variety of industries all over the world [1–6]. One of the most important characteristics of the chromium concerns its reactions to acids and bases as well as to air, a process known as oxidation. Some are the end product of a desired process but most of them are undesired byproducts known as disturb compounds [7–9].

Chromite is one of the most significant compounds used in steel industries [8–11]. The morphology of these compounds was also studied [12]. Earlier works showed that

two or three step reduction pathway of unsupported CrO<sub>3</sub> is or may be accompanied by simultaneous decomposition of intermediate CrO<sub>x</sub> phases (Cr<sub>3</sub>O<sub>8</sub> and Cr<sub>5</sub>O<sub>12</sub>), which are eventually transformed into crystalline Cr<sub>2</sub>O<sub>3</sub> at about 500 °C [13–17] of magnitude higher than the parabolic oxidation constant. Other experiments demonstrated that the presence of nitrogen in the substrate is always a precursor to breakdown of the oxide layer and does not result from diffusion through the Cr<sub>2</sub>O<sub>3</sub> layer [18].

The oxidation mechanism of chromium is of particular interest because it possesses a good high temperature oxidation resistance due to the protective character of the formed oxide scale. As a consequence, this element is widely used as an alloying element for commercial alloys, forming a rather protective oxide layer that prevents the underlying material from undergoing further degradation. Many studies on the formation of an oxide layer on pure chromium and chromium oxide-forming alloys have already been published, e.g. Refs. [19–27].

It is demonstrated that the oxidation behavior of chromium was significantly different according to the temperatures, i.e. 800, 900, and 1,000 °C. Under isothermal condition, the formation of a chromia scale on pure powder metallurgical chromium follows parabolic kinetics, indicative of a diffusion-controlled growth mechanism [26, 27]. In a previous work was studied the thermodynamic assessment of the Ni–O, Cr–O and Cr–Ni–O systems using the ionic liquid and compound energy models [26, 27].

In earlier investigation was CrO<sub>3</sub> subjected to thorough thermal analysis by means of TG and DTA [28].

The present research intended to investigate the thermal properties of chromium(VI) oxide under different temperature conditions. It is reported that pure chromium(III) oxide is the final product of thermal decomposition process for a number of different chromium compounds [29].

---

S. A. A. Sajadi (✉) · M. Khaleghian  
Institute of Water & Energy, Sharif University of Technology,  
P.O.Box 11365-8639, Tehran, Iran  
e-mail: sajadi@sharif.ac.ir

## Experimental

### Materials and equipments

Chromium (VI) oxide was purchased from Merck co., Darmstadt, Germany, artikel no. 64271.

Electrical furnace: Thermoline model 200, England.

XRD: X-Ray diffractometer STOE (Germany), Model: D-64295.

SEM: Scanning electron microscope, REM-JEOL (JXA-840), (Japan).

TG & DSC: Thermogravimeter/Differential Scanning Calorimeter, coupled with a TA processor, TGA/DSC1. Mettler-Switzerland.

Atomic Absorption Spectrometer, Spectra AA—Varian 220.

Spectrophotometer, Shimadzu, UV.

### TG and DSC analysis

A sample of  $\text{CrO}_3$  was placed in a standard aluminum crucible and weighed accurately (21.777 mg) using a microbalance. A special equipment was used to seal the sample. The sealed crucible was placed in the TG/DSC equipment and its temperature was raised from 25 to 600 °C, with a heating rate of 10 °C  $\text{min}^{-1}$ , under  $\text{O}_2$  and  $\text{N}_2$  gas atmospheres [30–35]. TG and DSC curves of this sample are represented in Figs. 1 and 2.

### X-ray powder diffraction

The product from TG/DSC experiment was prepared for X-ray and it was exposed to  $\text{CuK}_{\alpha 1}$  radiation for 2 h. Figure 3 shows the XRD diagram of the compound  $\text{Cr}_2\text{O}_3$ .

**Fig. 1** TG diagram of  $\text{CrO}_3$  in  $\text{N}_2$  (upper) and  $\text{O}_2$  (lower) atmospheres

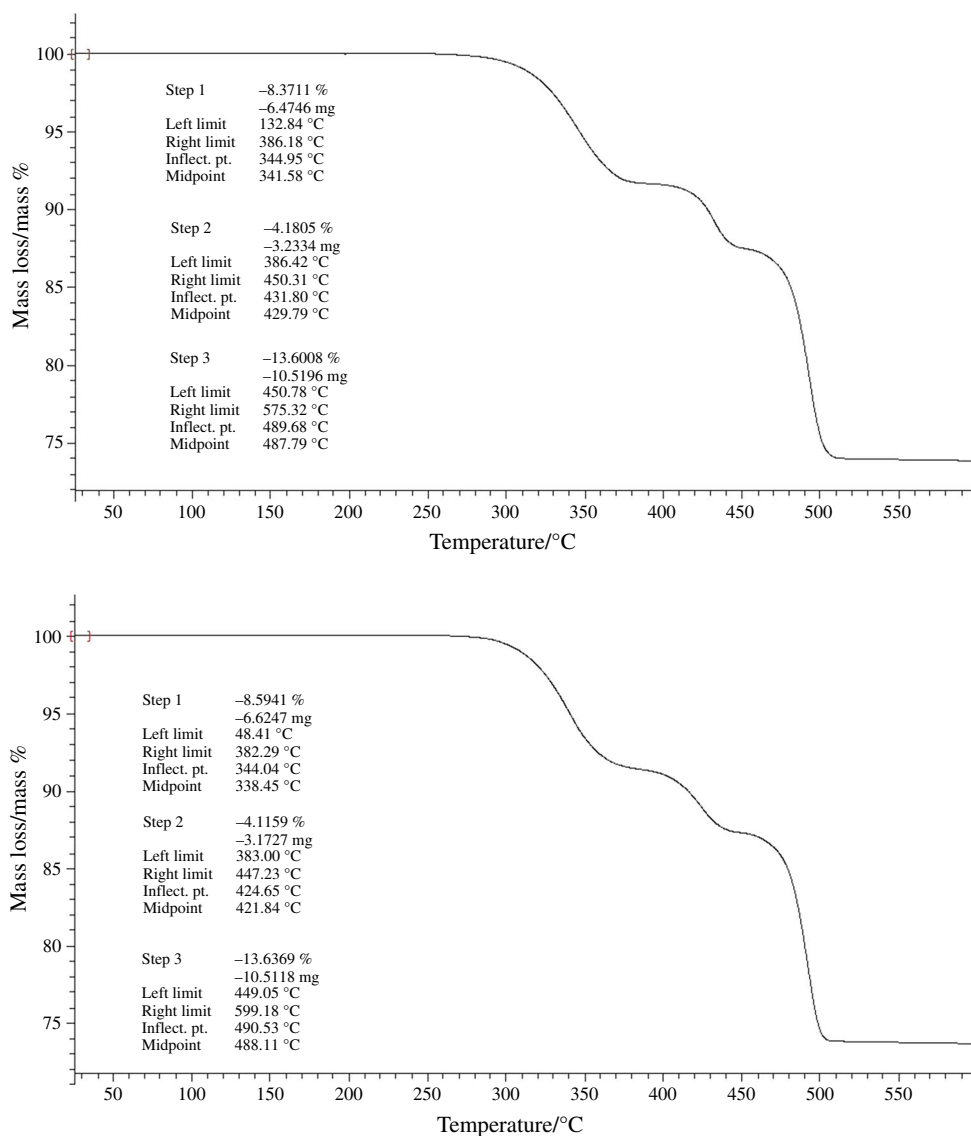
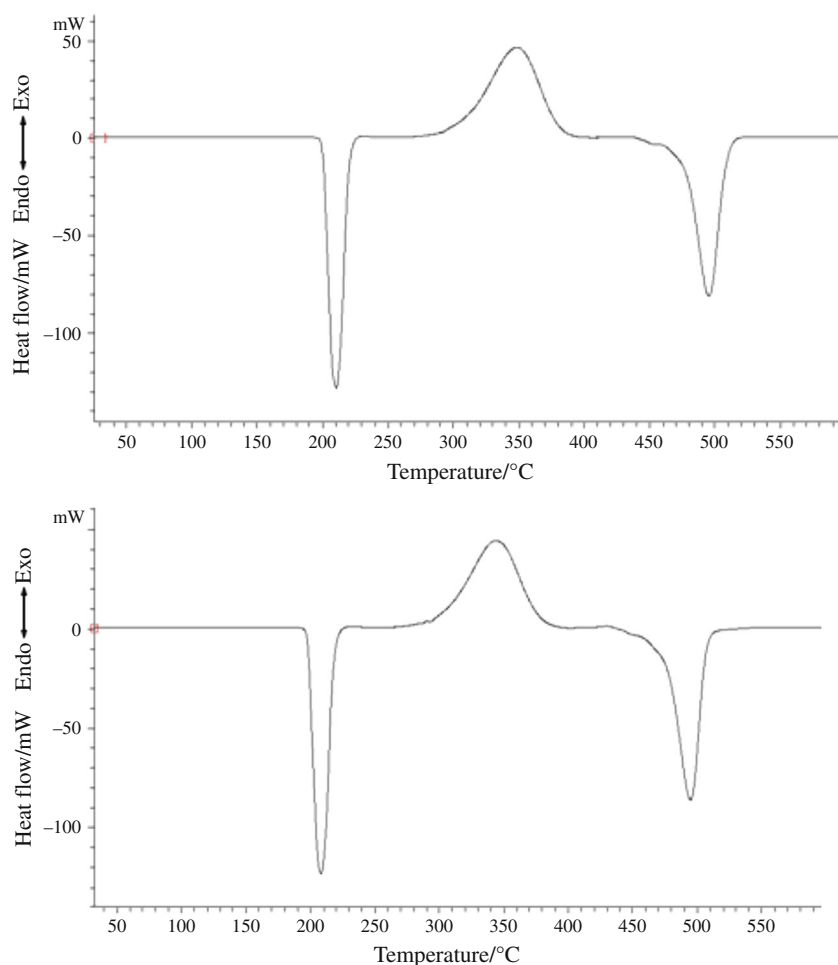


**Fig. 2** DSC diagram of CrO<sub>3</sub> in N<sub>2</sub> (upper) and O<sub>2</sub> (lower) atmospheres



### Electron microscopy (SEM)

The first series of the morphologic investigation of the product at 600 °C in O<sub>2</sub> and N<sub>2</sub> atmosphere was accomplished with a SEM electron microscope (REM-JEOL-JSM-840). The preparation of the sample was also accomplished by coating of the surface with gold (3–4 min). The reasonable enlargements were 1,000 times. The SEM photographs are shown in Figs. 4 and 5.

## Results and discussion

### Thermal investigations of CrO<sub>3</sub>

#### TG results

Both TG curves of thermal decomposition of CrO<sub>3</sub> in N<sub>2</sub> and O<sub>2</sub> atmosphere are shown in Fig. 1. The curve in the upper part shows the mass loss (vertical axis) of CrO<sub>3</sub> in N<sub>2</sub>

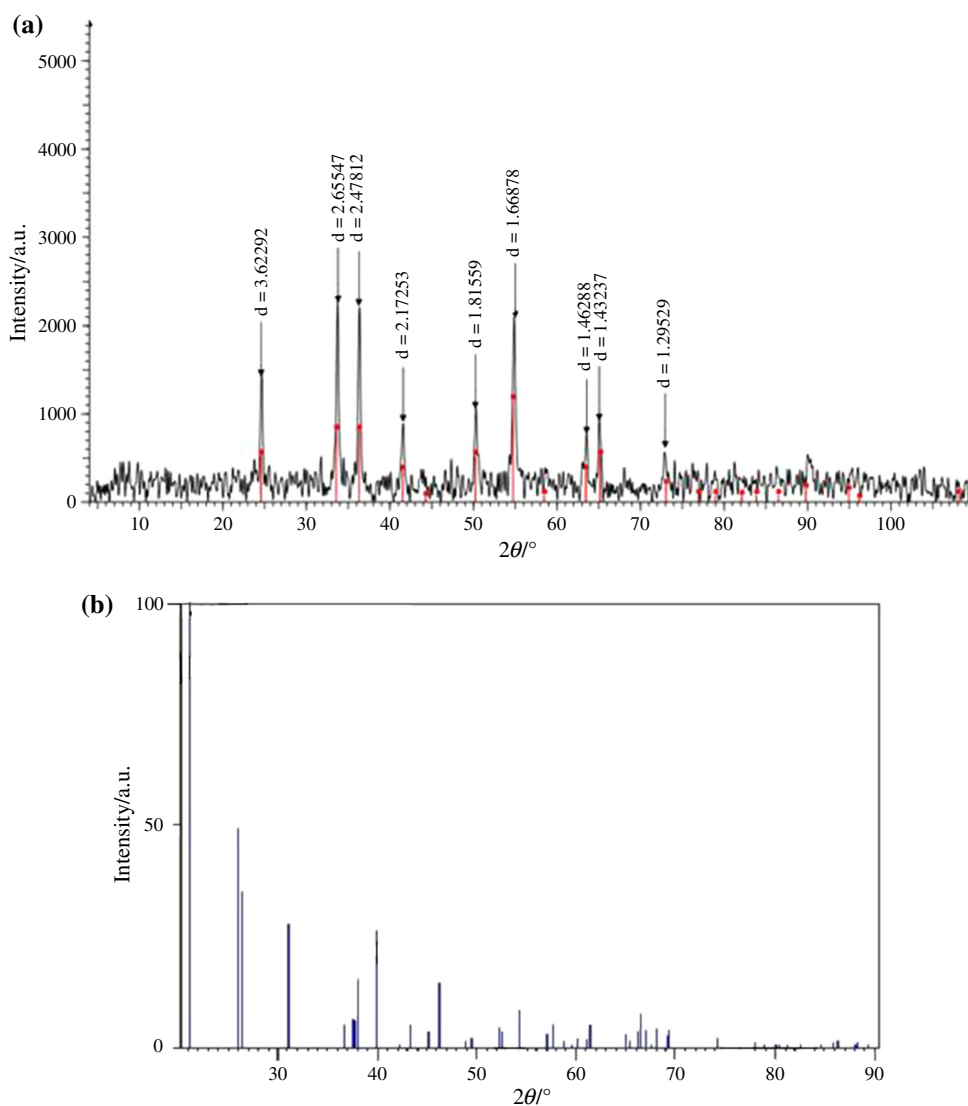
while horizontal axis shows temperature increase. The curve in the lower part shows the mass loss (vertical axis) of CrO<sub>3</sub> in O<sub>2</sub> while horizontal axis shows temperature increase.

So one can better differentiate between the steps of the thermal decomposition. The results indicate that thermal decomposition consists of three separate steps in the temperature range of 25–600 °C, these results are summarized in Table 1. Because of identical received results from experiments in N<sub>2</sub> and O<sub>2</sub> atmospheres, it is considered just the result of the first case.

The first step takes place between 132 and 386 °C. The calculations of mass loss show a chemical formula of Cr<sub>2</sub>O<sub>5</sub>. This phenomenon is the decomposition of the starting compound.

Spectroscopic quantitative analysis in this study also corroborates this finding. The computed stoichiometry of decomposition products are in good agreement with experimental results (quantitative and percent decrease in mass).

**Fig. 3** XRD diagram of  $\text{Cr}_2\text{O}_3$  (a) and  $\text{CrO}_3$  (b). File: Cr2mod.RAW – Type: 2Th/Th locked – start:3.998 – end:109.988 – step time: 1. S – Temp.: 25 °C (room) – time started: 0 s – 2-Theta:3.998 – Aux1:0.0 – Aux2:0.0 – Operation:smooth:0.150/ Background 1.000, 1.000/ Import. 01-1294(D) – Chromium Oxide –  $\text{Cr}_2\text{O}_3$  – Y:50.00 % - d x by: 1. – WL:1.5406 – Hexagonal (Rh) – a 4.95400 – b 4.95400 – c 13.66000 – alpha 90.000 – beta 90.000 – gamma 120.000 – primitive – R 3c (167) -2-290.331



#### First step of decomposition (132–386 °C)

A heating rate of  $10\text{ °C min}^{-1}$  was chosen to determine more information on what is taking place in this temperature range. The experiment was accomplished in the  $\text{O}_2$  atmosphere with a constant gas flow of  $30\text{ mL min}^{-1}$ .

As can be inferred from the results of the Fig. 1, the first phase of (decomposition) pyrolysis reaction of  $\text{CrO}_3$  occurs in the range of 132–386 °C. Concerning the case of  $\text{CrO}_3$ , the separation of  $\text{O}_2$  was also observed. Comparison of TG curves of  $\text{O}_2$  and  $\text{N}_2$  atmospheres for this step indicates the presence of the process i.e. loss of  $\text{O}_2$ .

By subtracting the experimentally determined quantity of materials (by spectrometric quantitative analysis) from the entire amount of mass loss (8.37 %), one can approximately compute the separated  $\text{O}_2$ -quantity and obtain the following formula:  $\text{Cr}_2\text{O}_5$ . X-ray investigation supplied an amorph XRD diagram to  $\text{Cr}_2\text{O}_5$ .

#### Second step of decomposition (386–450 °C)

The experiment results show that the product lost about 4.18 % of its mass within the range 386–450 °C. The experiment was accomplished in the  $\text{N}_2$  atmosphere with a constant gas flow of  $30\text{ mL min}^{-1}$ .

The X-ray analysis supplied an amorph XRD diagram. The evaluation of the results as well as spectrometric analysis confirms the brutto formula:  $\text{Cr}_2\text{O}_{4.5}$ .

#### Third step of decomposition (450–575 °C)

The third mass loss equals to about 13.6 % of the starting material and occurs in the temperature range of 450–575 °C. The X-ray analysis of the product confirms presence of  $\text{Cr}_2\text{O}_3$ . This was checked by spectrometric analysis and the calculated brutto formula of  $\text{Cr}_2\text{O}_3$  was obtained.

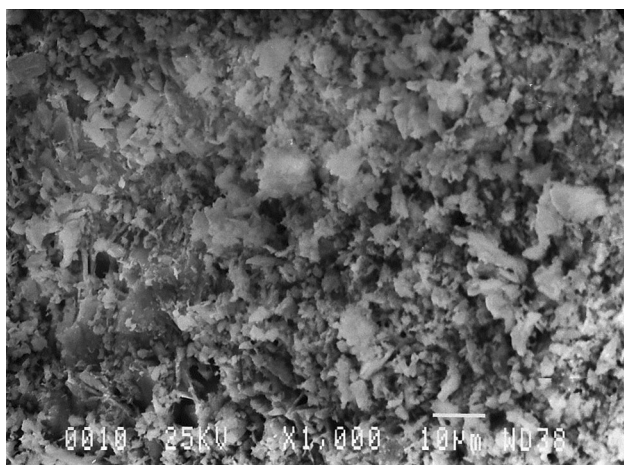


**Fig. 4** SEM electron microscopic photograph of Cr<sub>2</sub>O<sub>3</sub>, produces in O<sub>2</sub> atmosphere, enlargement is 1000×

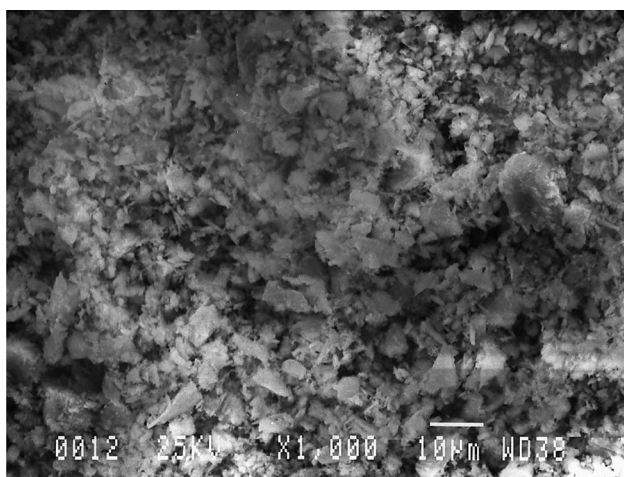


**Fig. 5** SEM electron microscopic photograph of Cr<sub>2</sub>O<sub>3</sub>, produces in N<sub>2</sub> atmosphere, enlargement is 1000×

**Table 1** results from the thermal investigations of CrO<sub>3</sub> in temperature range 25–600 °C in O<sub>2</sub> and N<sub>2</sub> atmosphere

Phase no.	Start temperature/°C	Turning point temperature/°C	End temperature/°C	Mass loss/mg	Mass loss/%
1	132.8	345	386.2	6.475	8.37
2	386.4	431.8	450.3	3.233	4.18
3	450.8	489.7	575.3	10.519	13.60

We want to point out again that the pyrolysis of CrO<sub>3</sub> within the range 25–600 °C in the N<sub>2</sub> and O<sub>2</sub>-atmosphere led to Cr<sub>2</sub>O<sub>3</sub>, i.e. the reaction CrO<sub>3</sub> → Cr<sub>2</sub>O<sub>3</sub> ran off completely with approximately 600 °C. From the above TG curve it is evident that the pyrolysis reaction of CrO<sub>3</sub> in the range 25–600 °C consists of three steps. The final decomposition product is Cr<sub>2</sub>O<sub>3</sub>.

**Table 2** DSC results, identification, and calculation of three peaks

No.	ΔH = Integral/mJ	Onset temperature/°C	Peak temperature/°C	Endset temperature/°C
1	−9,952.54	197.93	205.24	216.02
2	13.25e + 03	305.39	349.38	380.35
3	−10.91e + 03	475.13	491.82	506.55

If we compare the XRD diagrams of Cr<sub>2</sub>O<sub>3</sub> and CrO<sub>3</sub>, we obtain the change of start material to the product completely. There is no line of CrO<sub>3</sub> considerable (Fig. 3).

Therefore, the study of thermal behavior of CrO<sub>3</sub>, by TG suggests three different steps as discussed above. At first the compound loses oxygen in separate steps and changes from Cr(VI) to Cr(III). These changes occur at different temperatures and separate steps of thermal decomposition. These steps could be studied by using another technique (DSC) to determine the energy of each step. An earlier work showed that chromium trioxide decomposes in two steps. The first at about 220–375 °C, was accompanied by a 16 % mass loss, whereas the second, at 385–415 °C, brought the total mass loss up to 22.5 %. The corresponding DTG curve, revealed an endothermic process in the immediate vicinity of the first decomposition step at 200 °C, followed by a strong composite exothermic effect of three components, at 250, 330, and 390 °C. There was a second endothermic effect in a temperature range (465–500 °C) [28].

In contrast to above mentioned work we obtained three steps. The reason for this differences could be the flow gas, in above mentioned work was used air as flow gas. The other reason could be the heating rate (in last wok 5° min<sup>−1</sup>).

We received for the first and second intermediate products the formula Cr<sub>2</sub>O<sub>5</sub> and Cr<sub>2</sub>O<sub>4.5</sub>, but the XRD diagrams showed amorphous products, which we could not use for identification. The amorphous products indicate a disorganization of the former CrO<sub>3</sub> crystal lattice produced by a partially reduction of Cr(VI) to Cr(V) and/or Cr(IV).

## DSC results

Both exothermic and endothermic reactions are shown in Fig. 2. This heat flow can be either exothermic or endothermic. The energy is shown on vertical axis in mW and temperature is recorded on horizontal axis in °C. The TA processor was used to compute the enthalpy of an exothermic or endothermic reaction by entering the beginning and the termination point of each deflection. A straight or a sigmoid baseline can be selected which shows the change in Cp of a sample due to change in temperature. The surface area under each peak is computed automatically by the TA processor. The consequent results were  $H_{\text{exe}}$  or  $H_{\text{end}}$  in J g<sup>−1</sup>.

If we compare the TG and DSC results as Figs. 1 and 2 with each other we see that they confirmed each other.



DSC results of thermal decomposition of  $\text{CrO}_3$  are shown in Fig. 2 and Table 2. The first reaction shown in Fig. 2 is an endotherm and it starts at 198 and ends at 216 °C. The area under the peak was computed by TA processor. This reaction is represented more exactly in the Table 2. The maximum point of this reaction occurs at 205 °C. The  $\Delta H$  was 129.11 J g<sup>-1</sup>, or 12.91 kJ mol<sup>-1</sup>.

A second reaction occurs between 304.9 and 380.3 °C. This reaction is an exotherm. This part of the curve is considered more exactly in the Table 2. The area under the curve is computed. The maximum of this reaction is at 349.4 °C. The  $\Delta H$  for this peak is 178.45 J g<sup>-1</sup> or 17.845 kJ mol<sup>-1</sup>. The third peak (endothermic) starts at 475.1 and ends at 506.6 °C as shown in Fig. 2 which is considered more exactly in the Table 2. The maximum of this reaction is at 491.8 °C. The value of  $\Delta H$  was computed to be 141.53 J g<sup>-1</sup> or 14.153 kJ mol<sup>-1</sup>. These results confirm that the pyrolysis of  $\text{CrO}_3$  between 180 and 550 °C occurs in three separate steps (one exotherms and two endotherms).

If we use the entropy amount of the compound  $\text{CrO}_3$  (73.22 J K<sup>-1</sup> mol<sup>-1</sup>),  $\text{Cr}_2\text{O}_3$  (81.17 J K<sup>-1</sup> mol<sup>-1</sup>) [3], we received for the  $\Delta S$  of the following reaction: the value of 242.23 J K<sup>-1</sup> mol<sup>-1</sup>. Now we can use this value to calculate  $\Delta G$  for the compound  $\text{CrO}_3$  (611.30 kJ mol<sup>-1</sup>),  $\text{Cr}_2\text{O}_3$  (1,254.82 kJ mol<sup>-1</sup>), and for the above reaction 32.87 kJ mol<sup>-1</sup> [36]. The received experimental value for  $\Delta G$  in this work is also 29.30 kJ mol<sup>-1</sup>.

The XRD results obtained in this work is in a good agreement with standard diagram (ASTM 37-517) (Fig. 3) [37].

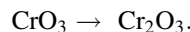
SEM photograph of produced  $\text{Cr}_2\text{O}_3$  at 600 °C in  $\text{O}_2$  atmosphere is shown in Fig. 4, crystals are foliated, tooth shaped with a diameter of 1–10 μm, they are arranged good next to each other and form large crystals. In Fig. 5 is shown the produced  $\text{Cr}_2\text{O}_3$  in  $\text{N}_2$  atmosphere at 600 °C. The crystals are tooth and leaf-shaped with a diameter of 1–10 μm, they are arranged good next to each other and form large crystals.

In previous work has been showed that the volatility diagram can be used to understand the possible etching reactions on the Cr–O system and reveal some effective methods for removal of  $\text{Cr}_2\text{O}_3$ -based passivating film [38]. The most important of these are (1) higher temperatures (100–400 °C), (2) oxidation of  $\text{Cr}_2\text{O}_3$  to  $\text{CrO}_3$  using ozone or atomic oxygen, followed by exposure of  $\text{CrO}_3$  to gaseous  $\text{H}_2$  or  $\text{HCl}$ . Regarding to this point please consider the conclusion of this work.

## Conclusions

Thermal behavior of  $\text{CrO}_3$  was examined using TG, DSC techniques, and following pathway was observed for the

thermal decomposition of  $\text{CrO}_3$ . After XRD experiments confirms the process of decomposition as well as identity of the final product  $\text{Cr}_2\text{O}_3$  at 550 °C



## References

- Ullmann. Encyclopedia of industrial chemistry (5. Auflage) "chromium and chromium alloys", vol. A7. Weinheim: VCH; 1986. p. 43.
- Gmelin. Handbook of inorganic and organometallic chemistry "chromium", vol. 52. Berlin: Springer; 1963.
- Greenwood N. Chemie der Elemente. Weinheim: Verlagsgesellschaft VCH; 1988. p. 440–53.
- Holleman AF, Wiberg E. Lehrbuch der anorganischen Chemie, vol. 101. deGruyter: Auglage; 1995.
- Khilla MA, Hanafi ZM, Mohamed AK. Physico-chemical properties of chromium trioxide and its suboxides. *Thermochim Acta*. 1982;59(2):139–47.
- Navrotsky A. Thermochemistry of chromium compounds, especially oxides at high temperature. *Geochim Cosmochim Acta*. 1975;39(6–7):819–32.
- Espinosa DCR, Tenório JAS. The case of healthcare waste and exhausted batteries. *Waste Manag*. 2001;21(4):405–10.
- Kittaka S, Morooka T, Kitayama K, Morimoto T. Thermal decomposition of chromium oxide hydroxide. *J Solid State Chem*. 1985;58(2):187–93.
- Oryshich IV, Poryadchenko NE, Rakitskii AN. High temperature oxidation of intermetallics formed by group IV transition metals with chromium. *Prot Met*. 2001;37(4):353–6.
- <http://www.mindat.org/min-1036.html> Mindat.org.
- John FP, Bruce RL. "Chromite". *Industrial minerals and rocks: commodities, markets, and uses*. 7th ed. Colorado: SME; 2006. ISBN 978-0-87335-233-8.
- Chandra V, Kumar A. *Spectrochim Acta Part A*. 2013;102:250–5.
- Józwiak WK, Ignaczak W, Dominiak D, Maniecki TP. Thermal stability of bulk and silica supported chromium trioxide. *Appl Catal A*. 2004;258(1):33–45.
- Barvinschi P, Barbu M, Stoia M, Stefanescu M. Evaluation of cation influence on the formation of M(II) $\text{Cr}_2\text{O}_4$  during the thermal decomposition of mixed carboxylate type precursors. *J Therm Anal Calorim*. 2013;112:359–66.
- Labus S, Malecki A, Gajerski R. Investigation of thermal decomposition of  $\text{CrO}_x$  ( $x \geq 2.4$ ). *J Therm Anal Calorim*. 2003;74:13–20.
- Udupa V. Solid state reactions in the system oxalate-bromate-chromium(III) oxide. *Thermochim Acta*. 1976;16(2):231–5.
- Soleimani E. Synthesis, spectral and thermal behavior of two novel complexes of Cr(III) with dibromobenziloxime. *J Therm Anal Calorim*. 2013;111:129–36.
- Royer L, Ledoux X, Mathieu S, Steinmetz P. On the oxidation and nitridation of chromium at 1300. *Oxid Met*. 2010;74:79–92.
- Jianian S, Longjiang Z, Tiefan L. High temperature oxidation of Fe–Cr alloys in wet oxygen. *Oxid Met*. 1997;48:347.
- Zurek Z. *Solid State Phenom*. 1995;41:185.
- Tveten B, Hultquist G, Norby T. Influence of hydrogen in some metals on aqueous-and gaseous corrosion. *Oxid Met*. 1999;51:221.
- Asteman H, Svensson JE, Johansson LG, Norell M. Hydrogen dissolution into 10 % chromium ferritic steels during high-temperature steam oxidation. *Oxid Met*. 1999;52:95.

23. Gleeson B, Harper MA. High temperature oxidation and corrosion of metals. *Oxid Met.* 1998;49:373.
24. de Asmundis C, Gesmundo F, Bottino C. *Oxid Met.* 1980;14:351.
25. Fox P, Lees DG, Lorimer GW. An investigation of growth mechanism of scale formatted on chromium. *Oxid Met.* 1991;36:491.
26. Buscaïl H, Jacob YP, Stroosnijder MF, Caudron E, Cueff R, Rabaste F, Perrier V. Structure and morphology studies of film at elevated temperature in hypersonic environment. *Mater Sci Forum.* 2004;461:93–100.
27. Taylor JR, Dinsdale AT. A thermodynamic assessment of the Ni–O, Cr–O, and Cr–Ni–O systems using the ionic liquid and compound energy models. *Z Metallkd.* 1990;81:354–66.
28. Zaki MI, Fahim RB. Thermal decomposition and creation of reactive solid surfaces. *J Therm Anal.* 1986;3(4):825–34.
29. Fouad NE, Halawy SA, Mohamed MA, Zaki MI. Kinetic and thermodynamic parameter of the decomposition of chromium chromate in different gas atmospheres. *Thermochim Acta.* 1999;32(1):23–9.
30. Sajadi SAA, Hashemian SJ. Study of Morphology of PbO. *J Sci A.Z.U.* 2001;14(2):25–31.
31. Sajadi SAA. Thermal behavior of lead acetate. *Sci Soc Appl Chem.* 2001;8:1–6.
32. Sajadi SAA. Study of thermal decomposition of PbCO<sub>3</sub> and their derivatives, their application in The industry. *J Sci T.U.* 2002;2:0.
33. Sajadi SAA, Hashemian SJ. Synthesis of Lead Hydroxide Carbonate 2Pb(OH)<sub>2</sub>·3PbCO<sub>3</sub> and investigation on the morphology and thermal properties. *Iran J Chem Chem Eng.* 2005;24:2.
34. Sajadi SAA, Alamolhoda, AA. Thermal analysis of Cr in different atmospheres. *Inorg Mat.* 2013 (in press).
35. Sajadi SAA, Alamolhoda AA, Hashemian SJ. Thermal behavior of alkaline lead acetate, a study of thermogravimetry and differential calorimetry. *Scientia Iranica.* 2008;15(4):435–9.
36. Kirklin DR. Review of previous thermodynamic property values for chromium and some of its compounds. *J Phys Chem Ref Data.* 1999;28(6):1675–704.
37. Yue W, Zhou W. Supplementary Material (ESI) for Journal of Materials Chemistry, This journal is (c) The Royal Society of Chemistry; 2007.
38. Hsieh M, Ge Y, Khan H, Michal M, Ernst F, Heuer AH. Volatility diagrams for the Cr–O and Cr–Cl systems: application to removal of Cr<sub>2</sub>O<sub>3</sub>-rich passive films on stainless steel. *Metall Mater Trans B.* 2012;43(5):1187–201.